ISSN 2723-6471

Progressive Massive Fibrosis Detection Using Generative Adversarial Networks and Long Short-Term Memory

Suhendro Y. Irianto[1,*], Sri Karnila[2], M.S. Hasibuan[3], Deshinta Arrova Dewi[4], Tri Basuki Kurniawan[5], Hendra Kurniawan[6]

[1,3,6]*Department of Informatics, Institute Informatics and Business Darmajaya, Pagar Alam No, 93, Lampung, Indonesia*

[2]*Department of Information System, Institute Informatics and Business Darmajaya, Pagar Alam No, 93, Lampung, Indonesia*

[4,5]*Faculty of Data Science and Information Technology, INTI International University, Nilai, Malaysia*

(Received: February 10, 2025; Revised: May 07, 2025; Accepted: August 01, 2025; Available online: September 01, 2025)

Abstract

Contribution: Progressive Massive Fibrosis (PMF) is a severe form of pneumoconiosis, affecting individuals exposed to mineral dust, such as coal miners and workers in the artificial stone industry. This condition causes significant pulmonary impairment and increased mortality. Early and accurate detection is vital for effective management, yet traditional diagnostic methods face challenges in differentiating PMF from other pulmonary diseases due to variability in clinical presentations and limitations in imaging techniques. Idea: The study introduces a novel diagnostic framework that integrates Generative Adversarial Networks (GAN) and Long Short-Term Memory (LSTM) networks to enhance the detection and monitoring of PMF. The GAN generates high-fidelity synthetic imaging data to address the issue of limited datasets, while the LSTM network captures temporal patterns in patient data, enabling real-time monitoring of disease progression. Objective: The primary objective of this research is to develop an AI-driven model that improves the accuracy and efficiency of PMF detection and monitoring, facilitating early diagnosis and better treatment planning. Findings: The integrated GAN-LSTM model significantly outperformed traditional diagnostic methods. It proved high accuracy, a Dice coefficient of 0.85, and an Area Under the Curve (AUC) of 0.92, showing precise differentiation of PMF from other pulmonary conditions, such as lung cancer and tuberculosis. Results: The GAN-LSTM framework achieved an accuracy of 91.3%, suggesting that the fusion of GAN and LSTM technologies can effectively address the challenges of limited datasets and heterogeneous disease progression. The model showed promise in enhancing the non-invasive detection and ongoing monitoring of PMF. Novelty: This research stands for a significant advancement in PMF diagnostics by combining GAN and LSTM technologies in a single framework. This approach improves diagnostic accuracy and eases continuous disease monitoring, offering a non-invasive and highly precise solution for PMF detection.

Keywords: AI-Driven Diagnosis, LST, GAN, PMF Pulmonary Disease

1. Introduction

Progressive Massive Fibrosis is the most severe form of lung disease linked to prolonged dust exposure, particularly chronic silicosis and CWP. According to [1], PMF is radiographically found by the presence of large opacities with a diameter of at least one centimeter. In silicosis cases, fibrotic masses are sometimes classified as PMF when their diameter reaches two centimeters or more. These masses, affecting lung tissue and bronchioles, can greatly compromise lung function. On chest X-rays, PMF can be mistakenly identified as carcinoma, tuberculosis, or infections caused by bacteria. Key consequence issues for PMF include exposure to high concentrations of inhalable coal dust or transparent silica, the incidence of smaller opacities, and a record of tuberculosis [2].

Recent reports by [3] There is a growing and urgent need for more correct models to detect PMF. Between 1970 and 2016, 4,679 cases of PMF were reported through the Black Lung Benefits Program, with more than half (2,474) occurring after 1996. This increase, particularly in recent decades, suggests that despite advancements in mining safety and medical monitoring, PMF stays a significant and possibly worsening health issue among coal miners. The concentration of cases in central Appalachia highlights regional disparities and the need for targeted early detection

***Corresponding author: Suhendro Y. Irianto (suhendro@darmajaya.ac.id)**
DOI: https://doi.org/10.47738/jads.v6i4.707

tools. Research from 2001 to 2013 writes down that severe PMF is more common among miners who began working after 1970, including younger workers (56 and younger) and elderly miners (80 and older). This underscores the limitations of current diagnostic methods and the need for advanced models, such as GAN-LSTM, to detect PMF earlier and more accurately.

Meanwhile, more information from the United States highlights the prevalence of CWP and PMF among various groups of coal miners, including those taking part in national physical condition observation programs. These findings reveal that PMF continues to be a significant and growing issue among coal miners. In 2015, more than 5% of alternative mine worker from mid Appalachia with at least 25 years of mining experience who participated in the national health investigation condition were diagnosed with PMF. A separate commentary concentrating on American Indian and Alaska Indigenous coalminers, primary [2]. In western United States, inspection conducted from 2014 to 2019 revealed that 3% of miners with at least 10 years of experience. Three studies have reported that pneumoconiosis, including PMF, also affects surface coal miners in the U.S., mainly showed radiographic evidence of pneumoconiosis, while 0.3% displayed findings consistent with PMF. Additional particularly those engaged in activities such as schooling, which involve exposure to inhalable crystalline silica, [4]. Moreover, the number of early-detected PMF cases is difficult to determine due to several factors, including underdiagnosis, differences in diagnostic criteria, and variability in reporting standards across regions and industries. In general, PMF is more often reported in populations with a significant history of coal dust or silica exposure, such as coal miners and workers in industries involving crystalline silica. To obtain more precise and up-to-date figures on early detected PMF cases, it is necessary to refer to recent epidemiological studies or health reports from occupational health organizations and government health agencies. These sources can provide specific statistics on the incidence and prevalence of PMF among exposed populations.

Predicting Progressive Massive Fibrosis is challenging due to the wide variation in how the disease presents and progresses in different patients. For example, some individuals may experience rapid lung function decline and severe breathlessness within a few months, while others may show only mild symptoms that progress slowly over several years. Additionally, some patients may respond well to certain treatments, while others do not improve at all. This clinical variability—seen in symptom severity, progression rate, and treatment response—makes it difficult to develop predictive models that perform consistently across diverse patient populations, [5], [6], [7], [8]. Additionally, medical data limitations and inconsistencies are often obstacles, as the data needed to train models is often incomplete or varies in quality and format. Environmental and genetic factors that influence PMF further complicate the issue, as specific and detailed data is needed to measure their impact. PMF diagnostics require advanced imaging techniques such as CT scans or MRIs, as well as in-depth clinical evaluations, which must be properly integrated into prediction models. Moreover, the rapid development of technology and algorithms requires models to stay updated with the latest techniques, posing a unique challenge. Model validation and generalization are also important, ensuring the model is tested across various populations to confirm its reliability in different clinical contexts, [2], [4], [9].

The aim of detecting Progressive Massive Fibrosis using Generative Adversarial Networks and LSTM is to improve the accuracy and efficiency of early identification and monitoring of the disease's progression. By combining GANs and LSTM, the detection system can use the power of deep image analysis and the ability to predict disease progression based on patients' historical data. This allows for faster and more accurate medical interventions, reduces the risk of misdiagnosis, and automates the process of analyzing medical data. Ultimately, this aims to create an advanced and holistic technological solution for PMF detection and management, which not only improves clinical outcomes but also enhances the quality of life for patients by enabling more personalized and proactive care [10], [11] [12], [13], [14] The urgency of this research on PMF is critical due to the severe impact it has on the health of people exposed to dust, particularly workers in the mining industry. PMF is an advanced form of pneumoconiosis that can lead to widespread scarring of lung tissue. The high risk of PMF is faced by people who are exposed to dust for prolonged periods. More in-depth research on risk factors, prevention, and treatment of PMF is needed to protect the health of these workers [15].

2. Related Works

The aim is to develop an automated model was developed to detect early-stage lung cancer using machine learning techniques. The model incorporates nine machine learning algorithms, including NB, LR, DT, RF, GB, and SVM. The performance of these classification algorithms was assessed using accuracy, sensitivity, and precision metrics derived from the parameters of a confusion matrix. The results showed that the proposed model achieved a maximum detection accuracy of 91%. Meanwhile, used support vector machines and applied techniques both with and without preprocessing [16]. According to the experimental results, decision trees yielded the most exact results, with an effectiveness of 90.24% without image processing, and with preprocessing, the best result was 82.43% effectiveness after image processing [17].

Furthermore [18], the models shown varying performance levels due to the intrinsic difficulty of the data, with precisions ranging from 0.77 to 0.85 and areas under the receiver operating characteristic curve between 0.85 and 0.94. Hybrid approaches that integrated dimensionality reduction with feature selection algorithms achieved the highest evaluation scores. Despite this, all machine learning models performed well, underscoring the potential of Raman spectroscopy as a robust tool for future in vitro lung cancer diagnostics, [19].Previous research also aimed to improve the accuracy of detection and speed up the process compared to earlier studies. According [20], proposed model, which is composed of seven convolutional layers, three pooling layers, and two fully connected layers for feature extraction. A Support Vector Machine (SVM) classifier was employed to classify nodules as benign or malignant. The experimental assessment was performed using the publicly available Lung Nodule Analysis 2016 as benchmark dataset. The proposed model achieved an accuracy of 87.64%, sensitivity of 86.37%, and specificity of 89.08%. Additionally, a comparative analysis was performed to evaluate the performance of the proposed Lung Net-SVM model against existing state-of-the-art methods for lung cancer classification.

PMF is one of the progressive diseases that is difficult to figure out precisely due to several factors, including a lack of diagnosis, differences in diagnostic criteria, and variations in reporting standards across regions and industries. In general, PMF is more often reported in populations with a significant history of exposure to coal dust or silica, such as coal miners and workers in industries involving crystalline silica, [4]. Research by [5], [21], [22] explained that that Progressive Massive Fibrosis with typical features is often misdiagnosed as lung cancer. While reports have described the typical characteristics of PMF, they often only include a brief review of the literature. They presented two cases of solitary PMF occurring without main simple pneumoconiosis or instant progression in a typical location, both of which were initially mistaken for lung cancer. According to [25], LSTM has memory cells and gate inputs (input gate, forget gate, cell gate, and output gate).

In forget gates, received data is treated, and the gate decides which information to preserve and which to abandon. It uses a sigmoid activation function, where a value of 1 show that the data is kept, and a value of 0 signifies that the data is discarded. The formula Eq. (1), is used for the forget gate [23], [24].

$$f_t = \sigma\left(W_f . [h_{t-1}, x_t] + b_f\right) \quad (1)$$

Next, in the input gate, two steps are taken: first, finding which values to update using the sigmoid activation function, followed by a tan function that creates new values stored in the memory cell. Eq. (2), (3) for the input gate is [14]:

$$i_t = \sigma(W_i . [h_{t-1}, x_t] + b_i) \quad (2)$$

$$\hat{c}_t = tanh(W_c . [h_{t-1}, x_t] + b_c) \quad (3)$$

Then, in the cell gate, the previous memory cell value is replaced with a new value by combining the values obtained from the forget gate and the input gate:

$$c_t = f_t * c_{t-1} + i_t * \hat{c}_t \quad (4)$$

Lastly, in the output gate, the memory cell value is selected using the sigmoid activation function, and the memory cell value is passed through the tanh activation function. The result of these two processes is multiplied to produce the final output:

 ISSN 2723-6471

$$o_t = \sigma(W_o.[h_{t-1}, x_t] + b_o) \quad (5)$$

$$h_t = o_t \tanh(c_t) \quad (6)$$

2.1. Generative Adversarial Networks

Generative Adversarial Networks are a deep learning framework where two neural networks compete to generate realistic data, such as creating new images from an image dataset or original music from songs, [11], [25]. As further explained by [26], the computational process is formed by complex mathematical equations, but here is a simplified explanation of how GANs work: The generator neural network analyses the training set and shows data attributes. The discriminator neural network also examines the original training data and independently distinguishes between various attributes. The generator introduces random variations to the data attributes, and the discriminator evaluates whether the generated output originates from the original dataset, providing feedback to help the generator refine the noise in next iterations.

The generator aims to increase the likelihood of errors made by the discriminator, while the discriminator focuses on minimizing these mistakes. Over multiple training iterations, both networks refine their performance, competing until they reach stability. At this point, the discriminator can no longer distinguish between real and generated data, signalling the end of the training process. GANs are considered adversarial because they involve training two networks that compete against each other. One network generates new data by changing the input data, while the other evaluates the authenticity of the generated data, continuously refining it until the discriminator cannot reliably tell real from fake, [11], [27].

The architecture of Generative Adversarial Network, a groundbreaking approach in AI and machine learning. The GAN consists of two neural networks: the Generator and the Discriminator. The Generator takes random noise (z) as input and generates synthetic data that closely resembles real samples. Both fake and real samples are then passed to the Discriminator, which classifies them as real or fake. The Discriminator calculates a loss value (discriminator loss) that reflects how well it distinguishes between the two. Simultaneously, the Generator minimizes its own loss (generator loss) to deceive the Discriminator. This iterative process refines both networks, resulting in highly realistic generated data.

However, despite its potential, the GAN-based approach for detecting PMF has several limitations. One significant challenge is mode collapse, a common issue in GAN training where the generator produces limited or repetitive outputs, reducing the diversity of synthetic images needed for robust model learning. Additionally, combining GANs with LSTM architectures demands high computational resources and prolonged training times, which can be impractical in clinical settings with limited infrastructure. The model's effectiveness also heavily relies on the quality and representativeness of the original dataset [12]. Moreover, stated by [28] that given the scarcity and variability of annotated PMF data, generating realistic and clinically meaningful synthetic images can be difficult. Furthermore, like many deep learning models, the GAN-LSTM approach lacks interpretability, making it challenging for healthcare professionals to trust or confirm its decisions. Ethical and legal concerns may also arise on the use of synthetic medical images, particularly in relation to patient privacy and data governance. Another risk is that the model may be overfit to artifacts introduced during data generation rather than learning clinically relevant features.

2.2. LSTM

According to [29] Recurrent Neural Networks (RNNs) have proven significant effectiveness in modelling dynamic systems that manage time- and sequence-reliant data, such as video, audio, and other sequential inputs. Long short-term memory, a specialized variant of RNN, incorporates state memory and a multilayer cell structure to enhance its performance. The hardware speeding up of LSTM with memristor paths has appeared as a growing research focus. This work examines the historical context and motivation behind the development of LSTM networks, provides a tutorial-style overview of existing LSTM methodologies, and highlights recent advancements in flexible LSTM architectures. Furthermore [13] said that the hyperparameters of all LSTM variants for each task were individually improved using random search, and their significance was evaluated through the robust functional Analysis of Variance (ANOVA) framework. In total, the study summarizes findings from 5,400 experimental runs (equivalent to approximately 15 years of CPU time), making it the largest investigation of its kind on LSTM networks. The study

 ISSN 2723-6471

shows that none of the LSTM variants significantly outperform the standard LSTM. It also highlights the forget gate and productivity initiation as key components, with hyperparameters being mostly independent.

To improve the LSTM model for PMF detection, key strategies applied to ensure effective learning from sequential image data. First, deep features are extracted from PMF images using a CNN such as ResNet or VGG. These features are then used as sequential inputs for the LSTM, preserving important spatial information. The LSTM architecture is carefully designed, often using a stacked or bidirectional LSTM (BiLSTM) to capture both past and future dependencies in the image sequences. The number of hidden units is tuned—typically ranging from 64 to 256—based on performance during validation, with dropout regularization applied between layers to prevent overfitting [14], [30], [31]. Hyperparameter tuning is crucial for improving model performance, involving adjustments to the learning rate, batch size, and sequence length using methods like grid search or Bayesian optimization. Learning rates are fine-tuned within a range of 0.001 to 0.00001 using adaptive optimizers. Batch size and time steps are designed for faster convergence and improved accuracy. The model is trained with binary or categorical cross-entropy loss and evaluated using metrics such as accuracy, Dice coefficient, and AUC.

The traditional LSTM network design, highlighting interactions among the cell state (Ct), hidden state (ht), and three gates: forget, input, and output. The forget gate (ft), governed by a sigmoid activation, decides which information to discard. The input gate (it) decides what current information to keep, updating the cell state with sigmoid and tanh activations. The output gate (Ot) selects relevant parts of the updated cell state, combining sigmoid and tanh functions to produce the hidden state (ht). [32], [33] . Moreover, it illustrates the internal structure of a LSTM cell, which is specifically designed to capture and keep long-term dependencies in sequential data. At the core of the LSTM is the cell state (Ct), a pathway that flows through the cell and allows information to be carried forward with minimal alterations. This mechanism enables the network to preserve memory over extended sequences. The LSTM cell uses three primary gates to regulate the flow of information: the forget gate, input gate, and output gate.

The forget gate (ft) finds which parts of the earlier cell state (Ct−1) should be discarded. It uses a sigmoid activation function, which takes as input the previous hidden state (ht−1h_{t-1}ht−1) and the current input (xtx_txt), and outputs values between 0 and 1—where 0 means "completely forget" and 1 means "completely retain."

The input gate (it) decides which current information should be added to the cell state. It uses a sigmoid function to decide which values to update and a tan function to generate candidate values (C~- ~t) to be added to the memory. The updated cell state is obtained by combining the retained information from the forget gate with the newly generated candidate values. Finally, the output gate (ot) determines the output of the LSTM unit. It uses a sigmoid activation to select parts of the updated cell state (Ct), which is then passed through a tan function to produce the new hidden state (ht). These gated mechanisms work together to allow the LSTM to manage long-term information and effectively model complex time-dependent patterns in data.

3. Methodology

3.1. Data Collection

The data used in this analysis will be obtained from a medical lung imaging dataset that includes patients diagnosed with PMF and lung cancer. This dataset, collected from Kaggle.com, has a total of 5,840 chest X-ray images: 624 for testing and 5,216 for training. The dataset included, Positive Cases (PMF): 1,500 images, Negative Cases (No PMF): 3,500 images. Training/Validation/Test Split: 70% training, 15% validation, and 15% testing. The data used in this analysis is sourced from a publicly available medical lung imaging dataset hosted on Kaggle.com, forming a total of 5,840 chest X-ray images. Of these, 5,216 images are distributed for training and validation, while 624 images are reserved for testing. The dataset includes two primary classes: positive cases (patients diagnosed with PMF), totaling 1,500 images, and negative cases (individuals without PMF), making up 3,500 images. The data is divided into training, validation, and testing sets using a 70:15:15 split. Although the dataset is moderately balanced, the higher number of negative samples may introduce class imbalance bias during model training, potentially leading to an overestimation of specificity.

3.2. Research Steps

This research conducted through several structured and systematic stages to ensure that every aspect of developing the detection model for PMF using GAN and LSTM is properly addressed. Below is a breakdown n of the stages that will be conducted. Figure 3 illustrates the stages of proposed method. Figure 3 illustrates a comprehensive series of stages for developing a robust detection model for PMF using deep learning. The process begins with a literature review to gather extensive references related to progressive disease imaging and earlier studies. This is followed by problem analysis to evaluate the significance of the research and show the methods and tools. Image data is sourced from Kaggle.com and undergoes preprocessing, which includes noise removal, handling of missing values, and normalization to ensure high data quality. The pre-processed data is then augmented to increase variability and enhance model generalization. Subsequently, the dataset is divided into training and testing subsets.

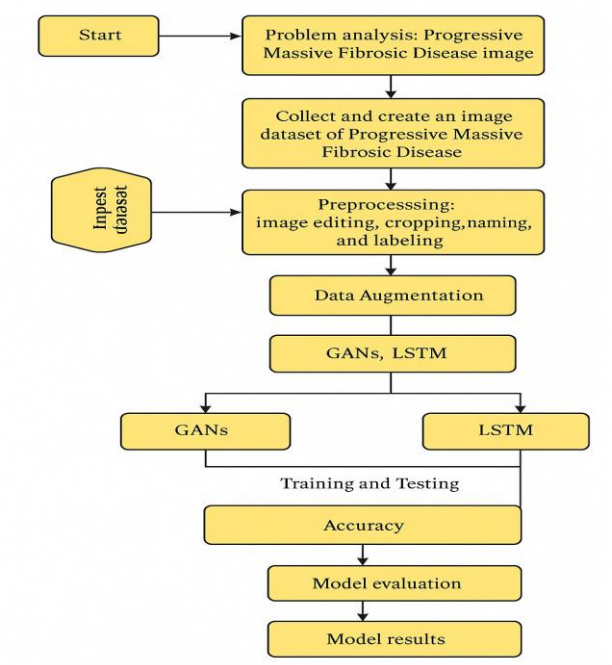

Figure 1. Research Steps

The model development phase GANs and LSTM networks, as shown in table 2. GANs are used to generate synthetic image data, enriching the dataset, while LSTMs capture temporal patterns, enhancing the model's ability to detect disease progression. After the model is built, it undergoes training and testing to assess its learning performance. Finally, the model is evaluated using various performance metrics, including accuracy, precision, recall, F1-score, and the area under the ROC curve (AUC). This structured workflow ensures a systematic and effective approach to developing a high-precision PMF detection model. Figure 1 outlines the research process, starting from dataset development and preprocessing to augmentation, GANs-LSTM training, evaluation, and result generation.

Figure 5 illustrates the training architecture, where the GAN's generator—integrated with LSTM layers—produces synthetic sequences from a noise vector. These are evaluated by a discriminator, also LSTM-based, which learns to distinguish between real and synthetic sequences. Both networks are iteratively trained using a loss function and backpropagation to improve generation and classification accuracy. The combined GAN-LSTM model is trained on both real and synthetic datasets and evaluated using metrics such as accuracy, AUC, and the Dice coefficient. This integrated approach enhances early-stage detection and reduces false negatives, offering a more dynamic and reliable method for PMF diagnosis. Ultimately, this model supports clinicians in improving early intervention and patient outcomes by leveraging both spatial and temporal patterns within the data.

This study introduces a novel approach for detecting Progressive Massive Fibrosis, a severe lung condition often caused by prolonged exposure to coal or silica dust. Early diagnosis is essential for effective treatment, yet conventional methods face limitations due to small datasets and the complex progression of the disease. To address these challenges,

 ISSN 2723-6471

the research integrates GAN and LSTM networks into a hybrid deep learning framework. GANs are employed to generate synthetic chest X-ray images, augmenting the limited real-world dataset. This synthetic data increases the diversity and volume of training samples, enabling the model to learn more robust visual features associated with PMF. Meanwhile, LSTM networks, known for processing sequential data, analyses the progression of fibrosis by evaluating image sequences or time-series clinical data. This allows the model to predict PMF development based on historical trends.

Figure 2 shows the proposed LSTM-GAN method generating sequential data from noise, classifying it, computing loss, and updating models. The GAN-LSTM model effectively addresses the diagnostic challenges associated with PMF by using its dual architecture to enhance both data generation and temporal prediction. Traditional diagnostic methods, such as radiography and CT scans, often struggle to differentiate PMF from visually similar conditions like lung cancer or tuberculosis due to overlapping radiographic features. The GAN part mitigates this issue by generating high-quality, synthetic imaging data, thereby enriching and diversifying the training dataset. This augmentation enables the model to learn more discriminative features specific to PMF, ultimately improving diagnostic accuracy.

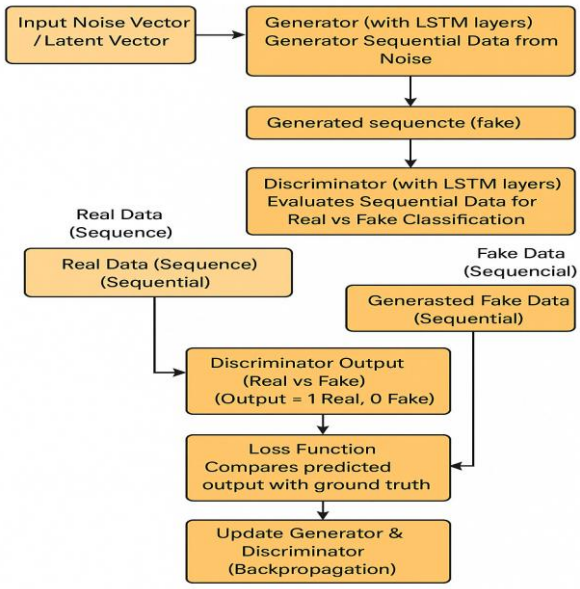

Figure 2. The Proposed Method

Additionally, the scarcity of annotated PMF datasets and the heterogeneity in disease progression hinder the development of dependable predictive models. The LSTM part addresses this challenge by capturing sequential patterns and temporal dependencies within patient data, allowing for a more nuanced understanding of disease progression. This temporal modelling is especially important for distinguishing PMF from other chronic pulmonary conditions that evolve differently over time. By combining the GAN's ability to generate diverse training data with the LSTM's strength in modelling time-dependent clinical features, the GAN-LSTM framework provides a robust solution that directly addresses the limitations of traditional diagnostic approaches—enhancing both the accuracy and generalizability of PMF detection [34].

4. Results and Discussion

4.1. Data Preprocessing

Dataset Preprocessing Steps are essential to prepare raw data for machine learning models, ensuring consistency, quality, and compatibility. The process typically involves the following key steps: resize and Normalization: Adjusting the image size to be uniform and normalizing pixel values. Editing and Cropping: Cropping images if there are specific requirements. Naming and Labelling: Preparing labels for images as either NORMAL or PNEUMONIA. An example of X-Rays images can be examined on figure 3.

 ISSN 2723-6471

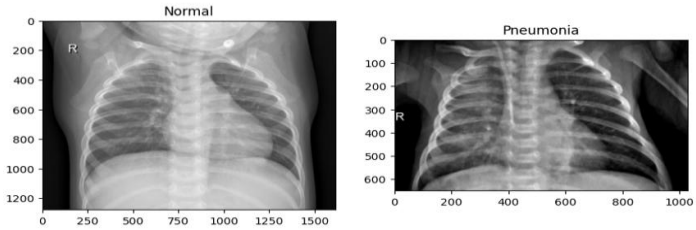

Figure 3. X-Rays Images

The purpose of data augmentation is to expand and enrich the dataset with variations of images produced through transformations such as rotation, flip, zoom, and other changes, without having to collect more data. Data augmentation will help make our model more robust and reduce overfitting. Below is the code for data augmentation using Image Data Generator. The data are trained with random transformations, such as rotation, shifting, and zooming, to make the model more generalized. Therefore, displaying examples of augmented data to ensure that the data variation is working properly. Figure 4 shows that more diverse training data was produced, which helped the model learn more effectively. When this approach works well, modeling can be continued using GANs and LSTM.

Figure 4. Augmented X-Rays Examples

This stage will build a Progressive Massive Fibrosis detection model using a combination of Generative Adversarial Networks to generate more varied data and Long Short -Term Memory to analyze the temporal development of the disease based on historical data. Figure 5, describes defining the architectures of GANs then combining them to create a complete model.

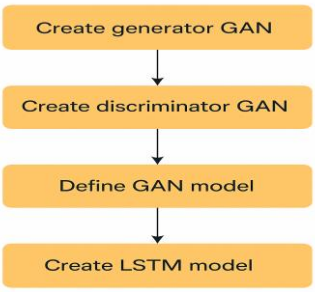

Figure 5. Integrating GAN and LSTM

Integrating GAN and LSTM, after creating GAN and LSTM separately, the next step is to integrate them effectively. GAN is used to generate other synthetic data to train LSTM in predicting disease progression based on image data. GAN generator produced synthetic images of lung disease, then LSTM processed sequence data from patients' historical data to predict the progression of PMF. Training and testing, this stage rained the Generator and Discriminator of the GAN, as well as train the LSTM to detect PMF based on augmented and pre-processed image data. Training GAN, it was trained slightly differently as alternately train the Generator and Discriminator. The Discriminator's task is to classify images as real or fake, while the Generator is trained to produce images that are challenging for the Discriminator to distinguish.

The GAN-LSTM architecture enhances PMF detection by combining data generation and temporal modelling. A random noise vector is input into a generator with LSTM layers, which produces synthetic sequential data resembling real patient data. This generated data, along with actual sequences, is fed into a discriminator—also equipped with

 ISSN 2723-6471

LSTM layers—that classifies the input as either real or fake. The output is compared with the ground truth using a loss function, and both networks are updated through backpropagation. Iterative training allows the generator to produce increasingly realistic data while the discriminator improves its classification accuracy. This approach enables data augmentation for limited PMF datasets and effectively captures temporal patterns in disease progression, offering a reliable, non-invasive method for early detection and monitoring of PMF [35].

The LSTM model has a total of 1,050,113 parameters, with 1,049,729 being trainable. These parameters are updated during training through backpropagation, enabling the model to learn complex patterns in time-series data. The high number of trainable parameters shows the model's ability to capture intricate relationships. However, the 384 non-trainable parameters suggest some fixed components, possibly related to specific layers or pre-trained embeddings. Figure 6 illustrates the large number of trainable parameters enhances learning, it also raises concerns about overfitting, necessitating the use of techniques like dropout, regularization, and data augmentation for better generalization.

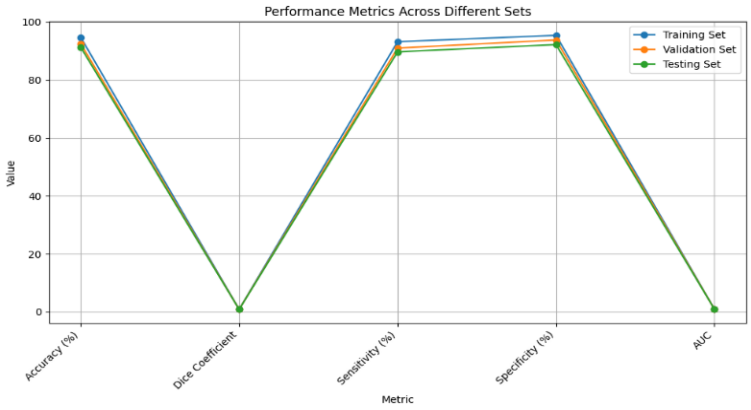

Figure 6. Metrices Performance

The models shows that the GAN-LSTM model outperforms the others, achieving the highest accuracy of 91.3%, an impressive Dice coefficient of 0.85, and the best AUC of 0.92. These results prove its superior performance in both classification and segmentation tasks. The CNN-LSTM model also performs well, with an accuracy of 88.3%, a Dice coefficient of 0.80, and an AUC of 0.88, showing strong ability to distinguish between classes and maintain solid segmentation overlap. The U-Net model, though slightly behind, achieves an accuracy of 86.5%, a Dice coefficient of 0.78, and an AUC of 0.86, showing solid performance with somewhat lower accuracy and segmentation quality. In conclusion, the GAN-LSTM model is the most robust, leading in all key performance metrics, followed closely by CNN-LSTM, while U-Net still shows strong overall performance.

Figure 7 illustrated a comparison of model performance across three dataset partitions—Training Set, Validation Set, and Testing Set—using five evaluation metrics: Accuracy, Dice Coefficient, Sensitivity, Specificity, and AUC. The model shows consistently high performance in terms of classification metrics, with accuracy, sensitivity, and specificity values all ranging between 90% and 95% across all datasets. This shows that the model generalizes well and is capable of accurately showing both positive and negative cases. However, the values for the Dice Coefficient and AUC are notably low, appearing close to zero across all sets. These unexpectedly low scores suggest potential issues with metric calculation or data visualization, particularly since they contradict the otherwise strong classification comment 4 performance.

4.2. Confusion Matrix

To judge the performing of a classification prototypical by summarizing its predictions and the actual outcomes in a structured table, providing comprehensive discernments the model's accuracy, errors, and types of misclassifications. The confusion matrix is particularly suitable for understanding the distribution of predictions across all classes, helping to diagnose issues with the model, such as class imbalance or bias.

Table 1 presents the model's performance metrics: 420 True Positives (TP), 35 False Negatives (FN), 50 False Positives (FP), and 495 True Negatives (TN). The model’s accuracy is 91.5%, calculated as (TP + TN) / (TP + TN + FP + FN). Precision, or positive predictive value, is 89.3%, writing down that 89.3% of predicted PMF cases are correct. Recall,

 ISSN 2723-6471

or sensitivity, is 92.3%, reflecting the model's ability to correctly name actual PMF cases. The F1 score, the harmonic mean of precision and recall, is 90.8%, proving balanced performance. Additionally, the performance of three deep learning models—CNN-LSTM, U-Net, and GAN-LSTM—was evaluated using accuracy, Dice coefficient, and AUC metrics. The GAN-LSTM model outperformed the others with the highest accuracy (91.3%), Dice coefficient (0.85), and AUC (0.92), followed by CNN-LSTM and U-Net.

Table 1. Confusion Matrix

	Predicted PMF	**Predicted to PMF**
Actual PMF	420 (true Positive)	35 (false Negative)
Actual No PMF	50 (false Negative)	495 (true Negative)

Table 1 also illustrates the model's performance metrics, emphasizing both its predictive accuracy and clinical relevance. The model correctly showed 420 patients with PMF, easing timely diagnoses and appropriate management. However, it misclassified 35 PMF patients as negative, potentially delaying treatment and worsening outcomes. Additionally, 50 individuals without PMF were incorrectly identified as positive, which could lead to unnecessary procedures and patient anxiety. On the positive side, 495 patients without PMF were accurately classified, minimizing overdiagnosis and unnecessary interventions. Overall, the model shows strong performance, balancing accurate detection with minimizing clinical risks.

4.3. Validation

The validation phase assessed the performance of three models—CNN-LSTM, U-Net, and GAN-LSTM—in detecting PMF. Based on the confusion matrix, the model achieved 580 TP and 835 TN, accurately naming PMF and No PMF cases. It reported 45 FN and 40 FP. With an accuracy of 94.33% (TP + TN divided by total predictions), the model demonstrated reliable performance. Precision was 93.55%, recall was 92.8%, and the F1 score reached 93.17%, showcasing a strong balance between sensitivity and precision. The results highlight the model's effectiveness in detecting PMF. Figure 7 comparing the validation metrics (accuracy, dice coefficient, and AUC) for the three models: CNN-LSTM, U-Net, and GAN-LSTM.

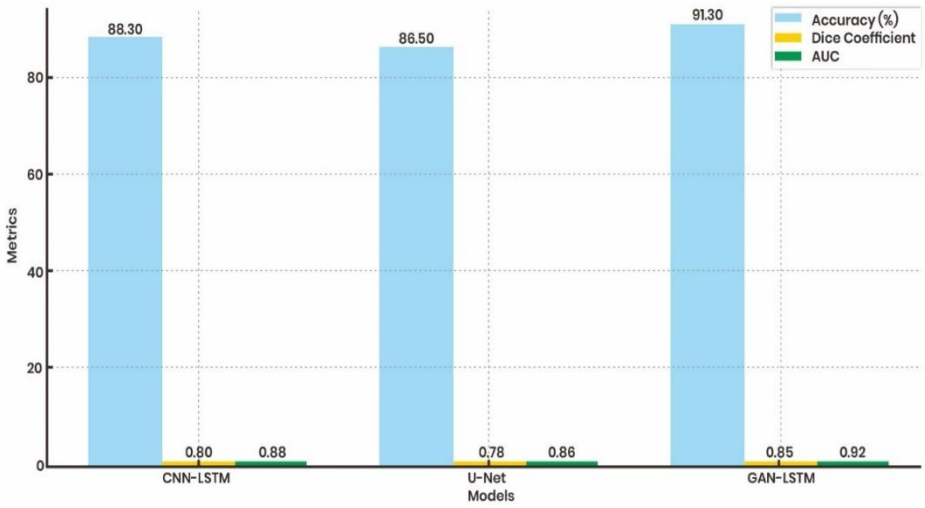

Figure 7. Validation Metrics of PMF Detection

This bar chart compares the performance of three machine learning models—CNN-LSTM, U-Net, and GAN-LSTM—across three metrics: Accuracy, Dice Coefficient, and AUC. GAN-LSTM achieves the highest performance in all metrics, with an accuracy of 91.30%, a Dice Coefficient of 0.85, and an AUC of 0.92. CNN-LSTM follows, reaching an accuracy of 88.30%, a Dice Coefficient of 0.80, and an AUC of 0.88. U-Net ranks the lowest among the three, recording an accuracy of 86.50%, a Dice Coefficient of 0.78, and an AUC of 0.86. Overall, GAN-LSTM outperforms the other models, proving superior effectiveness, while U-Net shows the weakest performance, particularly in Accuracy and Dice Coefficient.

 ISSN 2723-6471

Integrating Generative Adversarial Networks with Long Short-Term Memory networks offers a promising approach for detecting Progressive Massive Fibrosis. The GAN part generates synthetic lung disease images, augmenting the dataset and addressing data scarcity. These synthetic images are then used to train the LSTM model, which processes sequential patient data to predict disease progression. During training, the GAN's Generator and Discriminator are trained alternately: the Discriminator learns to differentiate between real and synthetic images, while the Generator aims to produce images that are challenging for the Discriminator to classify. This adversarial training enhances the quality of synthetic images. Subsequently, the LSTM model, including over a million parameters, is trained on this augmented dataset to capture temporal patterns in disease progression. Performance evaluations indicate that the GAN-LSTM model outperforms other architectures, achieving an accuracy of 91.3%, a Dice coefficient of 0.85, and an AUC of 0.92. These metrics suggest superior capability in both classification and segmentation tasks. The integration of GAN and LSTM thus provides a robust framework for PMF detection, using synthetic data generation and temporal analysis to enhance predictive accuracy. Compared to earlier works, our proposed method proves superior accuracy, as shown in table 2.

Table 2. Comparation three methods

Model	Accuracy (%)	Sensitivity (%)	Specificity (%)
Lung Net–SVM [18]	87.64	86.3	89.08
LSTM-GAN	93	91	94
SVM	91	N/A	N/A

Referring to table 2, the LSTM-GAN model proves the most robust performance among the models compared, achieving the highest accuracy of 93%, along with strong sensitivity (91%) and specificity (94%). These metrics highlight its superior ability to accurately classify both positive and negative cases, making it a highly reliable model for diagnostic applications. In contrast, the Lung Net–SVM model, while slightly lower in overall performance, still achieves a respectable accuracy of 87.64%, with sensitivity at 86.3% and specificity at 89.08%. This indicates balanced performance across both classes, though not as strong as the LSTM-GAN. The standard SVM model records an accuracy of 91%, which is notable; however, the lack of sensitivity and specificity metrics limits a comprehensive evaluation of its diagnostic effectiveness. The LSTM-GAN excels due to its combined strengths. LSTM networks effectively capture temporal dependencies, which are crucial for medical diagnostics. Meanwhile, GANs generate realistic synthetic data, addressing issues like class imbalance and limited datasets. By integrating LSTM's sequence modelling with GAN's data augmentation, the model enhances training diversity, improving generalization and diagnostic accuracy over traditional models.

5. Conclusion

Addressing the complexities of PMF requires a multidimensional approach that considers the disease's clinical variability, diagnostic challenges, and socioeconomic impacts. The integration of advanced machine learning techniques—particularly a hybrid GAN-LSTM model—offers a promising solution. The GAN-LSTM framework addresses these challenges by combining synthetic image generation with temporal pattern analysis. GANs are used to augment limited datasets by generating high-quality synthetic images, while LSTM networks capture sequential data patterns to monitor disease progression over time. This dual capability enhances both diagnostic precision and model robustness. The proposed model demonstrates strong performance, achieving an accuracy of 91.3%, a Dice coefficient of 0.85, and an AUC of 0.92. Beyond its technical advantages, early and accurate predictions using this model can reduce misdiagnoses, prevent unnecessary treatments, and support timely interventions—ultimately lowering healthcare costs and improving patient outcomes. This approach not only advances PMF detection but also contributes to more efficient, fair healthcare deliver.

To improve the clinical relevance of the proposed GAN-LSTM model for detecting PMF, future research should focus on several key areas. First, validation with larger, more diverse, and multi-center datasets is needed to ensure robustness across populations. Second, integrating clinical data—such as pulmonary function tests, exposure history, and lab results—can enhance the model's predictive power. Third, incorporating explainable AI techniques will improve interpretability and clinician trust. Finally, real-time deployment should be explored by developing lightweight,

scalable versions suitable for integration with radiology systems and use in low-resource or mobile healthcare environments.

6. Declarations

6.1. Author Contributions

Conceptualization: S.Y.I., S.K., M.S.H., D.A.D.; Methodology: S.Y.I., T.B.K.; Software: H.K.; Validation: S.K., T.B.K.; Formal Analysis: S.Y.I.; Investigation: D.A.D., H.K.; Resources: M.S.H., S.K.; Data Curation: H.K.; Writing – Original Draft Preparation: S.Y.I., D.A.D.; Writing – Review and Editing: S.K., M.S.H., T.B.K.; Visualization: H.K.; All authors have read and agreed to the published version of the manuscript.

6.2. Data Availability Statement

The data presented in this study are available on request from the corresponding author.

6.3. Funding

The authors would like to thank the Institute of Informatics and Business Darmajaya for providing l funding through the Institutional Grant Research scheme, as well as INTI International University for its support

6.4. Institutional Review Board Statement

Not applicable.

6.5. Informed Consent Statement

Not applicable.

6.6. Declaration of Competing Interest

The authors declare that they have no known competing financial interests or personal relationships that could have appeared to influence the work reported in this paper.

References

[1] Y. Shiwen, L. An, and S. Yuguo, “Analysis of the pulmonary function characteristics and associated factors in silicosis patients with progressive massive fibrosis,” *Chinese Journal of Industrial Hygiene and Occupational Diseases*, vol. 39, no. 11, pp.831-835, 2021, doi: 10.3760/cma.j.cn121094-20210507-00246.

[2] D. N. Weissman, “Progressive massive fibrosis: An overview of the recent literature, “PubMed”, *Pharmacology & Therapeutics*, vol. 240, no. Jun., pp.1-22, 2022. doi: 10.1016/j.pharmthera.2022.108232.

[3] S. R. Kang and J. Y. Rho, “Progressive Massive Fibrosis Mimicking Lung Cancer: Two Case Reports with Potentially Useful CT Features for Differential Diagnosis,” *Journal of the Korean Society of Radiology*, vol. 83, no. 5, pp.1175-1181, 2022, doi: 10.3348/jksr.2021.0185.

[4] .S. Sarı, A. Gökçek, A. Koyuncu, and C. Şimşek, "Computed tomography findings in progressive massive fibrosis: Analyses of 90 cases," *Med Lav.*, vol. 113, no. 1, pp. 1-20, Feb. 2022, doi: 10.23749/mdl.v113i1.12303. PMID: 35226653; PMCID: PMC8902743.

[5] M. Tang, F. Tan, Y. Luo, X. Xiao, X. Deng, S. Li, and X. Tan, "Tetrandrine slows the radiographic progression of progressive massive fibrosis in pneumoconiosis: a retrospective cohort study," *BMC Pulm. Med.*, vol. 23, no. 1, pp. 290-303, Aug. 2023, doi: 10.1186/s12890-023-02577-3. PMID: 37559034; PMCID: PMC10413607.

[6] S. Özgün, N. Zerman, G. Sarı, A. Koyuncu, C. Şimşek, F. Demirag, and S. U. Ramadan, "A case of lung cancer developing in the background of progressive massive fibrosis," *Respiratory Case Reports*, vol. 12, no. 3, pp. 109–113, 2023.

[7] A. Vangara, M. Gudipati, R. Chan, T. V. Do, O. Bawa, and S. S. Ganti, "Chronic pulmonary aspergillosis infection in coal workers pneumoconiosis with progressive massive fibrosis," *Journal of Investigative Medicine High Impact Case Reports*, vol. 10, no. Sep., pp. 1-4, 2022, Art. no. 23247096221127100, doi: 10.1177/23247096221127100.

[8] T. T. Tin, C. M. Chun, L. Y. Zhe, H. P. Tih, and C. M. Tze, “Non-image lung cancer prediction utilizing KNN model promoting health consciousness,” *International Journal of Innovative Research and Scientific Studies*, vol. 8, no. 1, pp. 2671–2679, 2025, doi: 10.53894/ijirss.v8i1.5040.

[9] N. Kanaji, N. Watanabe, T. Inoue, H. Mizoguchi, Y. Komori, Y. Ohara, and N. Kadowaki, "Immune checkpoint inhibitor-induced insidiously progressive, fatal interstitial lung disease," *J. Pers. Med.*, vol. 15, no. 3, pp. 115-127, Mar. 2025, doi: 10.3390/jpm15030115. PMID: 40137431; PMCID: PMC11943685.

[10] S. R. Rezaei and A. Ahmadi, "A GAN-based method for 3D lung tumor reconstruction boosted by a knowledge transfer approach," *Multimed Tools Appl*, vol. 82, no. 28, pp.44395- 44385, 2023, doi: 10.1007/s11042-023-15232-0.

[11] L. Tronchin, R. Sicilia, E. Cordelli, S. Ramella, and P. Soda, "Evaluating GANs in medical imaging," in *Deep Generative Models, and Data Augmentation, Labelling, and Imperfections (DGM4MICCAI DALI 2021)*, Lecture Notes in Computer Science, vol. 13003, Springer, Cham, 2021. https://doi.org/10.1007/978-3-030-88210-5_10 .

[12] R. D. Dhaniya and K. M. Umamaheswari, "CNN-LSTM: A Novel Hybrid Deep Neural Network Model for Brain Tumor Classification," *Intelligent Automation and Soft Computing*, vol. 37, no. 1, pp. 1129-1143, 2023, doi: 10.32604/iasc.2023.035905.

[13] M. Pradhan, I. L. Coman, S. Mishra, T. Thieu, and A. Bhuiyan, "LSTM based Modified Remora Optimization Algorithm for Lung Cancer Prediction," *International Journal of Intelligent Engineering and Systems*, vol. 16, no. 6, pp. 46-59, 2023, doi: 10.22266/ijies2023.1231.05.

[14] V. V. Kumar and P. G. K. Prince, "Gaussian Weighted Deep CNN with LSTM for Brain Tumor Detection," *SSRG International Journal of Electrical and Electronics Engineering*, vol. 10, no. 1, pp. 197-208, 2023, doi: 10.14445/23488379/IJEEE-V10I1P119.

[15] R. A. Cohen, C. S. Rose, L. Go, L. Zell-Baran, K. S. Almberg, E. Sarver, H. Lowers, C. Iwaniuk, S. Clingerman, D. Richardson, J. L. Abraham, C. Cool, A. Franko, A. Hubbs, J. Murray, M. Orandle, S. Sanyal, N. Vorajee, E. L. Petsonk, R. Zulfikar, and F. H. Y. Green, "Increased silica burden is associated with pathologic features of alveolar proteinosis, mature and immature silicotic nodules in US coal miners with progressive massive fibrosis (PMF) [abstract]," *Am. J. Respir. Crit. Care Med.*, vol. 205, no. 1, pp. 1-2, 2022.

[16] S. S. S. A. Siddiqui, R. T. S. H. Hyder, A. Manjaramkar and M. Jonnalagedda, "Automatic Detection of Lung Diseases Using CNN and SVM," *2023 3rd International Conference on Intelligent Technologies (CONIT)*, Hubli, India, vol. 2023, no. 1, pp. 1-5, doi: 10.1109/CONIT59222.2023.10205788.

[17] Z. Dai, Z. Wang, and J. Chen, "Progressive massive fibrosis in pneumoconiosis is mimicking lung malignancy on 18F-FDGPET-CT: two cases report," *Chinese Journal of Industrial Hygiene and Occupational Diseases*, vol. 40, no. 5, pp.1175-1183, 2022, doi: 10.3760/cma.j.cn121094-20210329-00170.

[18] A. M. Q. Farhan and S. Yang, "Automatic lung disease classification from the chest X-ray images using hybrid deep learning algorithm," *Multimed Tools Appl*, vol. 82, no. 25, pp. 38561-38587, 2023, doi: 10.1007/s11042-023-15047-z.38561–38587.

[19] J. Song et al., "Korean clinical imaging guidelines for the appropriate use of chest MRI," *Journal of the Korean Society of Radiology*, vol. 82, no. 3, pp. 562-574, 2021, doi: 10.3348/JKSR.2020.0185.

[20] I. Naseer, S. Akram, T. Masood, M. Rashid, and A. Jaffar, "Lung Cancer Classification Using Modified U-Net Based Lobe Segmentation and Nodule Detection," *IEEE Access*, vol. 11, no. 1, pp. 60279-60291, 2023, doi: 10.1109/ACCESS.2023.3285821.

[21] L. Riley and D. Urbine, "Chronic silicosis with progressive massive fibrosis," *N. Engl. J. Med.*, vol. 380, no. 23, pp. 1-22, Jun. 2019, doi: 10.1056/NEJMicm1809675. PMID: 31167054.

[22] S. R. Kang and J. Y. Rho, "Progressive massive fibrosis mimicking lung cancer: Two case reports with potentially useful CT features for differential diagnosis," *J. Korean Soc. Radiol.*, vol. 83, no. 5, pp. 1175–1181, Sep. 2022, doi: 10.3348/jksr.2021.0185. PMID: 36276214; PMCID: PMC9574288.

[23] S. Altun and A. Alkan, "LSTM-based deep learning application in brain tumor detection using MR spectroscopy," *Journal of the Faculty of Engineering and Architecture of Gazi University*, vol. 38, no. 2, pp. 1139-1148 1202, 2023, doi: 10.17341/gazimmfd.1069632.

[24] S. Ayub, R. Kannan, S. Ragadeesh, S. Shitharth, R. Alsini, T. Hasanin, and C. Sasidhar, "LSTM-based RNN framework to remove motion artifacts in dynamic multicontrast MR images with registration model," *Wireless Communications and Mobile Computing*, vol. 2022, no. 1, 12 pp., 2022, doi: 10.1155/2022/5906877.

[25] M. Jeong, D. Kim and J. Paik, "Practical Abandoned Object Detection in Real-World Scenarios: Enhancements Using Background Matting With Dense ASPP," in *IEEE Access*, vol. 12, no. 1, pp. 60808-60825, 2024, doi: 10.1109/ACCESS.2024.3395172.

[26] L. Hong, M. H. Modirrousta, M. H. Nasirpour, M. M. Chargari, F. Mohammadi, S. V. Moravvej, L. Rezvanishad, M. Rezvanishad, I. Bakhshayeshi, R. Alizadehsani, I. Razzak, H. Alinejad-Rokny, and S. Nahavandi, "GAN-LSTM-3D: An

 ISSN 2723-6471

efficient method for lung tumour 3D reconstruction enhanced by attention-based LSTM," *CAAI Transactions on Intelligence Technology*, vol. 2023, no. May, pp. 1–10, 2023.

[27] José Mendes, Tania Pereira, Francisco Silva, Julieta Frade, Joana Morgado, Cláudia Freitas, Eduardo Negrão, Beatriz Flor de Lima, Miguel Correia da Silva, António J. Madureira, "Lung CT image synthesis using GANs," *Expert Syst Appl*, vol. 215, no. 1, pp. 535-542, 2023, doi: 10.1016/j.eswa.2022.119350.

[28] S. Najari, M. Salehi, and R. Farahbakhsh, "GANBOT: A GAN-based framework for social bot detection," *Social Network Analysis and Mining*, vol. 12, no. 1, pp. 1-4, 2022, doi: 10.1007/s13278-021-00800-9. PMID: 34804252; PMCID: PMC8590628.

[29] K. Smagulova and A. P. James, "A survey on LSTM memristive neural network architectures and applications," *The European Physical Journal*, vol. 2288, no. 10, pp. 2313–2324 , 2019. doi: 10.1140/epjst/e2019-900046-x.

[30] S. Y. Irianto, R. Yunandar, M. S. Hasibuan, D. A. Dewi, and N. Pitsachart, "Early Identification of Skin Cancer Using Region Growing Technique and a Deep Learning Algorithm," *HighTech and Innovation Journal*, vol. 5, no. 3, pp. 640–662, Sep. 2024, doi: 10.28991/HIJ-2024-05-03-07.

[31] K. Saranya, U. Karthikeyan, A. S. Kumar, A. O. Salau, and T. Tin Tin, "DenseNet-ABiLSTM: Revolutionizing Multiclass Arrhythmia Detection and Classification Using Hybrid Deep Learning Approach Leveraging PPG Signals," *International Journal of Computational Intelligence Systems*, vol. 18, no. 1, pp. 1-19, Dec. 2025, doi: 10.1007/s44196-025-00765-z.

[32] S. Akila Agnes, J. Anitha, and A. Arun Solomon, "Two-stage lung nodule detection framework using enhanced UNet and convolutional LSTM networks in CT images," *Comput. Biol. Med.*, vol. 149, no. Oct., pp. 1-22, Oct. 2022, doi: 10.1016/j.compbiomed.2022.106059. PMID: 36087510.

[33] H. Imaduddin, L. A. Kusumaningtias, and F. Y. A'la, "Application of LSTM and GloVe Word Embedding for Hate Speech Detection in Indonesian Twitter Data," *Ingenierie des Systemes d'Information*, vol. 28, no. 4, pp. 1107-1112 , 2023, doi: 10.18280/isi.280430.

[34] R. Wakamoto, S. Mabu, S. Kido, and T. Kuremoto, "Anomaly Detection of Lung Sounds Using Deep Neural Networks ー Comparison and Improvement of the Performance of DAGMM and Efficient GAN ー," *IEEJ Transactions on Electronics, Information and Systems*, vol. 142, no. 12, pp. 496-504, 2022, doi: 10.1541/ieejeiss.142.1328.

[35] N. V. R. Reddy et al., "Enhancing Skin Cancer Detection Through an AI-Powered Framework by Integrating African Vulture Optimization with GAN-based Bi-LSTM Architecture," *International Journal of Advanced Computer Science and Applications*, vol. 14, no. 9, pp. 559-572, 2023, doi: 10.14569/IJACSA.2023.0140960.